# Molecular Z-Scheme for H$_2$ Production via Dual Photocatalytic Cycles

Photoexcitation of both an aryl alcohol and a photocatalyst in the presence of an e$^-$ donor lead to catalytic H$_2$ generation.

*Pooja J. Ayare,[1,†] Noelle Watson,[2,†] Maizie R. Helton,[1] Matthew J. Warner,[1] Tristan Dilbeck,[2] Kenneth Hanson,[2,*] Aaron K. Vannucci[1,*]*

[1]Department of Chemistry and Biochemistry, University of South Carolina, Columbia, SC 29208, USA

[2]Department of Chemistry & Biochemistry, Florida State University, Tallahassee, FL 32306, USA

†P.J.A and N.W. contributed equally.

[*]corresponding authors: vannucci@mailbox.sc.edu, hanson@chem.fsu.edu

**Abstract:** Natural photosynthesis uses an elaborate array of molecular structures in a multi-photon Z-scheme for the conversion of light energy into chemical bonds (i.e. solar fuels). Extensive research effort has been dedicated to achieving artificial photosynthesis but a fully molecular artificial Z-scheme for solar fuels production has yet to be realized. Here we show that upon excitation of both a molecular photocatalyst (PC) and an aryl alcohol (ROH) in the presence of a sacrificial electron donor and proton source, we achieve artificial photosynthesis of H$_2$. Chemical, electrochemical, and spectroscopic data support a mechanism consisting of: 1) photoexcitation of PC, 2) reduction of excited state PC, 3) electron transfer from PC$^-$ to photoexcited ROH, and 4) generation of H$_2$ from reduced ROH. The system is catalytic with respect to both PC and ROH and operates at a reaction overpotential of ~40 meV. This molecular Z-scheme circumvents the thermodynamic and overpotential constraints associated with reduction of weak acids in their ground-state and offers a new paradigm for the conversion of light energy into H$_2$ bond energy.

## Introduction

The conversion of solar energy into chemical bond energy via photosynthetic organisms is the foundation of life on earth. Given its ubiquity and utility, considerable efforts are underway to realize efficient "artificial" photosynthesis[1-3] that harnesses solar energy for the production of chemical fuels such as hydrogen (H$_2$) to meet the energy consumption needs of humans.[4] The inherent thermodynamic driving forces combined with reaction overpotentials[5] make it difficult to form chemical bonds with the energy of a single photon that is typically absorbed by photosynthetic chromophores.[6] Nature circumvents this limitation by using a Z-Scheme (Figure 1, left) which combines the energies of two independent light absorption events to drive chemical bond breaking/making.[7, 8]
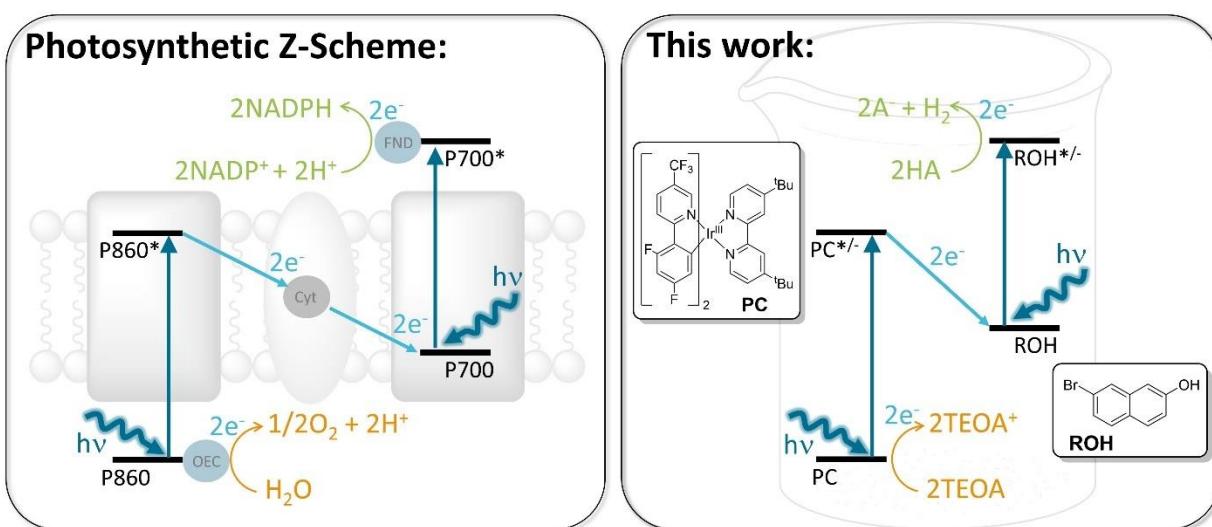
For both natural and artificial photosynthetic systems, there are stringent thermodynamic requirements that must be met for chemical fuels generation. For example, the minimum energy required to generate H$_2$ from a weak acid is dependent on the p$K_a$ of the acid (p$K_{a,HA}$) as described in equation 1:

$$E_{HA}^o = E_{H+}^o - \frac{2.303RT}{F} pK_{a,HA} \quad (1)$$

where $E°_{HA}$ is the reduction potential of the weak acid in its ground-state, $E°_{H^+}$ is the thermodynamic potential required to reduce a proton in a given solvent, R and F are the gas and Faraday's constants respectively, and T is the temperature.[9] Consequently, the thermodynamic minimum for the reduction of weak acids in acetonitrile solution is between -0.3 to -1.5 eV versus the saturated calomel electrode (SCE). Furthermore, experimental results consistently show that an additional overpotential energy between 0.1 and 1.0 eV are necessary,[5, 10] even for platinum metal catalysts.[9, 11] Thus, Z-schemes require photon

energies much greater than the thermodynamic reduction potentials in order to achieve $H_2$ production at reasonable rates.(*4*) Designing a catalytic $H_2$ generation scheme that efficiently exploits excited-state electron transfers for the reduction event could minimize reaction overpotentials and would represent a breakthrough in solar energy conversion.(*12*)

There has been progress in developing Z-schemes for artificial photosynthetic systems using a variety of approaches including multijunction solar cells, quantum dots, and tandem dye-sensitized photoelectrosynthesis cells.(*13-20*) These artificial Z-schemes are composed of inorganic (i.e. semiconductor based) light absorbing/charge transport materials and often require additional, optically inactive, transition metal catalysts to perform the bond breaking/making reactions. While the transition metal catalysts are used to help minimize reduction overpotentials, overpotentials of > 0.1 eV are still commonly observed.(*13*) Judicious construction of the systems is also necessary to ensure proper charge transfer and redox reactivity. To date, however, a fully molecular based artificial Z-scheme for converting solar energy to chemical bonds has yet to be realized.



**Figure 1**. A simplified depiction of the natural photosynthetic Z-scheme (left), and the molecular Z-scheme reported here (right). TEOA = triethanolamine, HA = weak acid.

Here we show that upon excitation of both a photocatalyst (PC) and an aryl alcohol (ROH) in the presence of a sacrificial electron donor and a proton source results in the photocatalytic generation of $H_2$. The proposed dual catalytic cycle consists of reduction of excited state PC ($PC^* + e^- \rightarrow PC^-$), electron transfer from $PC^-$ to the excited ROH ($PC^- + ROH^* \rightarrow PC^- + ROH^-$), followed by the production of $H_2$. Regeneration of ROH can also be achieved with phenol (PhOH) as the sacrificial proton source ($RO^- + PhOH \rightarrow ROH + PhO^-$). This "molecular Z-scheme" (Figure 1, right) circumvents the thermodynamic and overpotential constraints associated with reduction of weak acids in their ground-state and offers a new paradigm for the conversion of light energy into $H_2$ bond energy.

**Results and Discussion**

To realize a molecular Z-scheme, 7-bromo-2-naphthol (ROH) was chosen as a photon-absrobing aryl alcohol proton source due to its long-lived triplet excited state ($\tau_{^3ROH^*} = 15$ μs; Figure S4) that enables diffusion limited, bimolecular reactions.(*21*) Also, in the ground state, ROH has a relatively high reduction potential ($E^o_{red} = -1.39$ V vs SCE in MeCN) and is only weakly acidic ($pK_a = 27.9$ in MeCN) such that it is

unfavorable for direct reduction of ROH to ROH[-] and/or H^{+} to $H_2$ by common reduction photocatalysts (see SI for more details). Ir(dF-CF$_3$-ppy)$_2$(dtbpy)[+], where dF-CF$_3$-ppy is 2-(2,4-difluorophenyl)-5-(trifluoromethyl)pyridine and dtpby is 4,4′-tertbutyl-2,2′-bipyridine, was chosen as the photocatalyst (PC) due to its long triplet excited-state lifetime ($\tau_{^3PC*}$ = 2.2 µs; Figure S5) and its excited-state oxidation potential is thermodynamically below the reduction potential of the ground state of ROH.(*22*) Lastly, triethanolamine (TEOA) was used as the sacrificial electron donor because its potential is favorable for the reduction of $^3PC*$ but not $^3ROH*$.

With system design in hand, broadband irradiation of an MeCN solution containing 100 mM ROH, 150 mM TEOA, and 2.5 mol% PC (0.07 mmols) for six hours resulted in 0.16 mmol of $H_2$ corresponding to a turnover number (TON) of 4.5 and 0.1 for the PC and ROH, respectively. While these initial TONs are modest, the results confirm the ability of the system to photocatalytically produce $H_2$, with respect to the PC, without the need for an additional, optically transparent, transition metal catalyst to promote the hydrogen bond making reaction.(*23*)

To investigate the mechanism of this reaction, a series of control experiments were performed, and the results are summarized in Table 1. Three different light conditions were used 1) broadband light (200-700 nm) capable of exciting both PC and ROH, 2) blue light (400-500nm) that can excite PC but not ROH (Figure S6), and 3) in the dark where no photoexcitation is occurring. Only with broadband light capable of exciting both the PC and ROH was a measurable quantity of $H_2$ observed (entry 1, Table 1). The lack of $H_2$ generation under blue light (entry 2) and in the dark (entry 3) implies that both the PC and ROH must be excited for the reaction to occur.

**Table 1.** Summary of various reaction conditions and the resulting quantity of $H_2$.[a]

| | Reaction Condition | | | | | Product Outcome | | |
|---|---|---|---|---|---|---|---|---|
| Entry | [PC] (mM) | [ROH] (mM) | [TEOA] (mM) | Light[b] | Other | mmol $H_2$[c] | TON$_{PC}$[d] | TON$_{ROH}$[e] |
| 1 | 2.5 | 100 | 150 | Broadband | - | 0.16 | 4.5 | 0.1 |
| 2 | 2.5 | 100 | 150 | Blue | - | 0 | 0 | 0 |
| 3 | 2.5 | 100 | 150 | - | - | 0 | 0 | 0 |
| 4 | 2.5 | 100 | - | Broadband | - | 0 | 0 | 0 |
| 5 | - | 100 | 150 | Broadband | - | 0 | 0 | 0 |
| 6 | - | 100 | - | - | 100 mM PC[-] | 0 | 0 | 0 |
| 7 | - | 100 | - | Broadband | 100 mM PC[-] | 0.42 | 0.3 | 0.3 |
| 8 | 2.5 | - | 150 | Broadband | - | 0.03 | 0.9 | N/A |
| 9 | - | 100 | - | - | 3.08 mM K | 0.95 | N/A | 0.7 |
| 10 | 2.5 | - | 150 | Broadband | 100 mM MCA | 0.06 | 1.6 | N/A |
| *11* | *2.5* | *10* | *150* | *Broadband* | *100 mM PhOH* | *1.50* | *42.9* | *10.7* |
| 12 | 2.5 | - | 150 | Broadband | 100 mM PhOH | 0.08 | 2.3 | N/A |

[a]Reaction vessel contained 28 mL of acetonitrile and 3.5 mL of $N_2$ purged headspace. [b]450W Hanovia Hg lamp (Broadband) or 34 W Kessil H150 (Blue). [c]All reactions performed in at least duplicate and mmol of $H_2$ are reported with ±5% accuracy. [d]TON with respect to PC. [e]TON with respect to ROH.

Selective removal of TEOA (entry 3) or PC (entry 4) resulted in no measurable quantities of $H_2$ suggesting that PC* and its reduction product by TEOA (i.e. PC[-]) are necessary events in the catalytic solution. To gain further insights into the role of PC[-] and ROH, PC[-] was prepared by chemical reduction

with potassium and then stirred with ROH in the dark for 6 hours (entry 6). GC analysis showed no $H_2$ production suggesting that $PC^-$ does not reduce ground-state ROH or produce $H_2$ directly. However, a mixture of $PC^-$ and ROH under broadband irradiation for 6 hours resulted in similar $H_2$ production ($TON_{ROH}$ = 0.3, entry 7) to the complete reaction ($TON_{ROH}$ = 0.1, entry 1). In addition, electrochemical measurements using an indium tin oxide electrode modified with PC(24) under reducing bias (-0.4 V vs. SCE) gave minimal photocurrent response (<10 µA) (Figure S7). Upon the addition of ROH, however, switchable photocurrents of >15 µA were observed indicating that ROH* can serve as an electron transfer relay in the electrolyte solution (i.e. $PC^-$ + ROH* → $PC^-$ + $ROH^-$). Collectively these results suggest that the formation of $PC^-$ and photoexcitation of ROH are necessary for $H_2$ production in this catalytic system.

As an aside, it is worth noting that a small but measurable amount of $H_2$ was produced from a solution containing just PC and TEOA (i.e. without ROH, entry 8). This $H_2$ production most likely occurred from chemical decomposition of the oxidized TEOA.(25) This is an important observation because TEOA is a commonly used sacrificial electron donor in photocatalytic $H_2$ producing systems,(26) however we were unable to find a report that considered TEOA as a source for $H_2$. Regardless, in the current study, the amount of $H_2$ from TEOA was negligible compared to the system containing $PC^-$ and ROH* indicating that TEOA is not necessary for the production of $H_2$.

We envisioned two possible pathways for the photocatalytic generation of $H_2$ from $PC^-$ and ROH*: the reduction of ROH* by $PC^-$ to generate $ROH^-$, followed by $H_2$ production (eq 2) or the generation of acidic protons by ROH* (eq 3) that are then reduced by $PC^-$ (eq 4).

$$2ROH^* + 2e^- \rightarrow 2ROH^- \rightarrow H_2 + 2RO^- \quad (2)$$

$$2ROH^* \rightarrow 2RO^- + 2H^+ \quad (3)$$
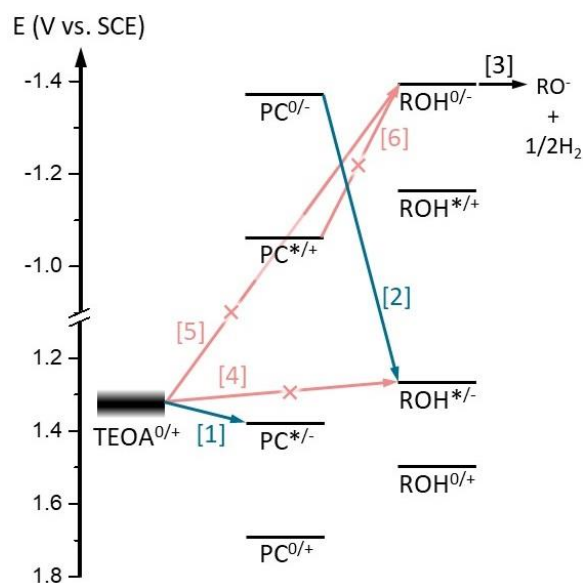
$$2H^+ + 2e^- \rightarrow H_2 \quad (4)$$

To investigate a possible bimolecular reaction between $ROH^-$ molecules to generate $H_2$, ROH was chemically reduced with potassium metal (Table 1, entry 9) and significant $H_2$ production (0.95 mmol) was observed with the primary organic product being $RO^-$ (Figure S9). This corresponds to a nearly 70% conversion of the protons from ROH to $H_2$. Furthermore, kinetic studies under chemical reduction conditions showed that $H_2$ production scaled linearly with the concentration of ROH to the second power, consistent with a second order reaction with respect to ROH. Electrochemical reduction of ROH was also monitored with UV-visible absorption spectra, and a clear isosbestic point for the conversion of ROH to $RO^-$ (Figure S8) was observed. This result indicates that the bimolecular reaction that generates $H_2$ is rapid in comparison to the experimental time frame as $ROH^-$ was not observed. These experiments are consistent with the mechanism proposed in equation 1, but do not necessarily rule out the photoacid mechanism shown in eq 3 and 4.

Naphthol and its derivatives are known transient photoacids with notably increased acidities in the excited state.(27) Following excitation and $^3ROH^*$ formation, the $pK_a$ of ROH decreases from 27.9 (in MeCN) to 16.4 as determined from a Förster cycle analysis (see SI for details).(28-30) This transient acidity increases the $H^+$ concentration in solution (eq 2) which could be followed by the reduction of $H^+$(eq 3). To test the role of solution acidity in $H_2$ production, chloroacetic acid (MCA, $pK_a$ = 15.3) was used as a surrogate for $^3ROH^*$. Under standard reaction conditions 0.06 mmol $H_2$ was produced from 100 mM MCA (entry 10), which is nearly three-fold lower than the solution containing ROH (entry 1). It is important to note that the effective concentration of $^3ROH^*$ is <0.1 mM because it is limited by photon flux and the excited state lifetime, and thus the $H^+$ concentration for a solution containing 100 mM ROH is many orders of magnitude lower than for 100 mM MCA. Consequently, the low $H_2$ production from MCA indicates that

solution acidity plays a minimal role in $H_2$ production from the catalytic solution. Instead, ROH* is acting as an electron acceptor/shuttle which then facilitates $H_2$ formation via a bimolecular reaction between ROH- (eq 1). This observation opens interesting opportunities for aryl alcohol molecules to serve as the chemical, electrochemical, and/or photochemical catalysts for the production of $H_2$.

It is worth note that the catalytic production of $H_2$ from excitation of a brominated naphthol containing solution has been observed before.(*29*) In that report, the authors proposed that the excited state photoacidity of 6-bromo-2-naphthol was sufficient to protonate a well-known cobalt-diglyoxime secondary catalyst, followed by $H_2$ generation.(*31, 32*) However, their "anomalously large" rate constant for the proposed protonation(*29*) and the results above suggest that reduction of excited 6-bromo-2-naphthol by Co[I]-diglyoxime followed by $H_2$ generation may have been an operable reaction mechanism in their study.

Collectively the above results are consistent with the energy level diagram depicted in Figure 2. Photon absorption by PC is followed by reductive quenching of $^3$PC* by TEOA to generate PC- ([1] in Figure 2). A photon is also absorbed by ROH, and the resulting $^3$ROH* is reduced by PC- [2]. ROH- molecules then undergo a rapid bimolecular reaction to generate $H_2$ and RO- [3]. Electron transfer events 4-6 in Figure 2 are thermodynamically unfavorable and not observed. The net reaction is the reduction of ROH by TEOA to generate $H_2$, which cannot occur in the ground-state or by ROH excitation alone. The reaction is made energetically accessible via the excitation of both PC and ROH, analogous to the Z-scheme of photosynthesis. This cooperative strategy puts less energetic restrictions on the catalyst and light harvesting components enabling new design strategies for solar fuels formation.



**Figure 2**. Energy level diagram for TEOA, PC, and ROH with energetically favorable and unfavorable processes depicted by blue and red arrows, respectively. Excited state potentials are for triplet excited states (i.e. $^3$PC* and $^3$ROH*).

As described above, irradiation of a solution containing PC, ROH, and TEOA results in the photocatalytic production of $H_2$ and RO-. That reaction, however, is only catalytic with respect to PC, and not ROH, and will stop when ROH is consumed. To regenerate ROH during the catalytic reaction, phenol (PhOH) was added as a sacrificial proton source. Broadband irradiation of an acetonitrile solution
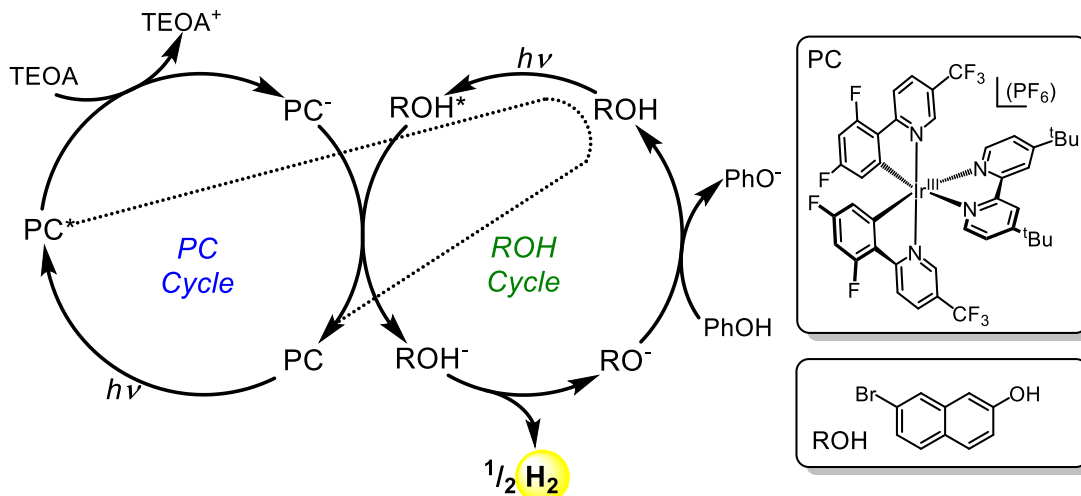
containing 2.5 mM PC, 10 mM ROH, 100 mM PhOH, and 150 mM TEOA resulted in the formation of 1.5 mmols of $H_2$ which corresponds to a TON of 42.9 with respect to the PC and 10.7 with respect to ROH (Table 1, entry 11). Removal of ROH from the reaction (entry 12) resulted in a nearly 20-fold decrease in $H_2$ indicating that PhOH is not solely responsible for the $H_2$ increase, and $^3$ROH* is needed for high $H_2$ production. Thus, upon regeneration, ROH becomes both a proton shuttle and a photocatalyst in the reaction.

The p$K_a$ of PhOH(9) and ROH in MeCN are 27.2 and 27.9, respectively. Consequently, the acid-base equilibrium constant (equation 5) indicates that PhOH to $RO^-$ proton transfer is favorable.
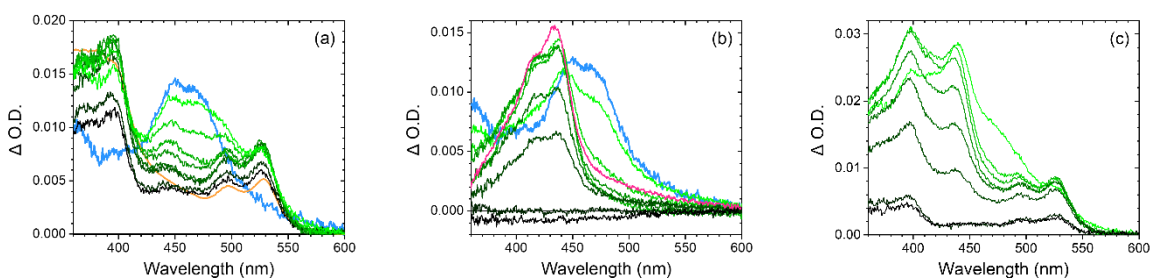
$$RO^- + PhOH \rightleftharpoons ROH + PhO^- \qquad K_{eq} = 5.0 \qquad (5)$$

Furthermore, $^1$H NMR spectra of a solution containing $RO^-$ and PhOH shows the formation of ROH and confirms that PhOH can protonate $RO^-$ (Figure S9-11). This regeneration step closes the catalytic cycle with respect to ROH and results in a dramatic increase in TON$_{ROH}$. The regeneration of ROH from $RO^-$ may also prevent homoconjugation between ROH and its conjugate base ($RO^{-...}H-OR$), an interaction that is known to impede catalytic $H_2$ generation.(33, 34)

The proposed photocatalytic mechanism for the production of $H_2$ from a solution of PC, ROH, TEOA, and PhOH is shown in Figure 3. This reaction generates $H_2$ from the relatively unreactive TEOA and PhOH, a thermodynamically unfavorable process by 2.65 eV, but is enabled by the additive effects of two independent excitation events in a dual catalytic Z-scheme. Furthermore, the highest energy electron generated ($ROH^-$) has an energy of only 0.04 eV above the thermodynamic potential required to reduce PhOH. Thus, this molecular Z-scheme minimizes the overpotentials associated with catalytic $H_2$ production.



**Figure 3**. Proposed mechanism for the catalytic generation of $H_2$ from PhOH and TEOA in molecular Z-scheme consisting of two independent light absorption cycles.

Further support for the mechanism in Figure 3 is provided by transient absorption spectroscopy (TA); the key results are shown in Figure 4. Two different excitation wavelengths were used: 375 nm for the excitation of PC and 335 nm for excitation of both PC and ROH (Figure S6).

**Figure 4**. Transient absorption spectra of a) PC and TEOA (1:10; $\lambda_{ex}$ = 375 nm) with $^3$PC* (at 5 ns) in blue and the chemically generated PC$^-$ spectrum in orange, b) PC and ROH (1:10; $\lambda_{ex}$ = 375 nm) with $^3$PC* and $^3$ROH* (at 5 ns) in blue and red, respectively, and c) PC, TEOA, and ROH (1:20:10; $\lambda_{ex}$ = 335 nm) in MeCN. Time slices progress from green to black at 0.005, 0.5, 1.0, 2.0, 5.0, 10.0, 100, and 1000 μs.

Upon 375 nm excitation of a MeCN solution containing only PC and TEOA (Figure 4a), there is a rapid (<1 μs) decrease in the $^3$PC* feature (425-500 nm, Figure S5) followed by the formation of a structured absorption spectra resembling that of the chemically generated PC$^-$ via reduction with potassium. This is consistent with the previously reported reductive quenching reaction, $^3$PC* + TEOA $\rightarrow$ PC$^-$ + TEOA$^+$, that occurs with a near diffusion limited Stern-Volmer quenching constant of $7 \times 10^8$ M/s (Figure S15).(*22*)  The resulting PC$^-$ lifetime is significantly longer than our acquisition time window (>1 ms). In contrast, the excited state decay of $^3$ROH* ($\tau \approx 15$ μs) was unperturbed by the addition of TEOA.

For an acetonitrile solution containing just PC and ROH, excitation of only the PC at 375 nm (Figure 4b) resulted in a TA spectral shift consistent with the $^3$PC* to ROH triplet energy transfer with a Stern-Volmer quenching constant of ~$8 \times 10^9$ M/s (Figure S16). Importantly, in Figure 4b there are no indications of the formation of PC$^+$/PC$^-$ or an increased rate of $^3$ROH* decay (375-475 nm) demonstrating that no redox events are occurring and that $^3$PC* to ROH energy transfer is the only excited state interaction upon sole excitation of the PC. Excitation of both PC and ROH at 335 nm (Figure S17) resulted in a similar $^3$PC* to $^3$ROH* spectral evolution, but with a larger initial contribution from $^3$ROH* ($\lambda_{max} \approx 440$ nm) from direct excitation of ROH. Interestingly, although this triplet sensitization mechanism (dashed line in Figure 3) is competitive with the formation of PC$^-$, it is still a productive pathway as it also generates the reactive $^3$ROH* species.

In a solution containing PC, ROH, and TEOA, 335 nm excitation was again followed by the rapid disappearance of $^3$PC* feature, but now with the sustained presence of PC$^-$ and $^3$ROH* spectral signatures (Figure 4c) consistent with the mechanistic steps at the top of the catalytic cycles in Figure 3. Similar results were observed with 375 nm excitation (Figure S18) presumably through the triplet sensitization mechanism (the dashed line in Figure 3). Concomitant decay for PC$^-$ ($\lambda_{max} \approx 370$ nm) and $^3$ROH* ($\lambda_{max} \approx 440$ nm) occurs with a lifetime of ~10 μs which is faster than the intrinsic decay of PC$^-$ ($\tau$ >1 ms) and $^3$ROH* ($\tau \approx 15$ μs) suggesting a cooperative decay mechanism. Based on the results above, we attribute this cooperative decay to reduction of $^3$ROH* by PC$^-$. We observed no spectral features that would be indicative of ROH$^-$ formation, which is also consistent with the electrochemical reduction of ROH where H$_2$ generation was the rapid step.

Collectively, these spectroscopic results are consistent with the mechanism in Figure 3 which was proposed based on the experiments in Table 1 and the electrochemical data. The spectroscopic studies also indicate that $^3$ROH* generation via $^3$PC* sensitization can occur, effectively making this a tri-catalytic reaction solution but with the sensitization process being redundant and less efficient than direct excitation of ROH. Nonetheless, with sufficient blue photon flux we anticipate that $H_2$ generation could occur via the $^3$PC* to ROH triplet sensitization step, but minimal $H_2$ was observed under our excitation conditions (35 W blue LED).

**Conclusions**

Here we report the realization a molecular Z-scheme for the photocatalytic production of $H_2$. This solar fuels generating reaction is achieved by concurrent excitation of a molecular photocatalyst and an aryl alcohol in the presence of an amine electron donor and a phenol proton source. A series of chemical and electrochemical control reactions support a dual catalytic mechanism that exploits two excited-state electron transfer reactions involving the photocatalyst and aryl alcohol, with the net reaction being reduction of phenol by triethanolamine to generate $H_2$. Transient absorption measurements further support this proposed mechanism and give evidence for a third catalytic cycle involving triplet energy transfer from the photocatalyst to the aryl alcohol. In addition to being a first of its kind, an entirely molecular artificial Z-scheme, this system operates under remarkably low reaction overpotentials ($\leq 0.04$ eV), thus illustrating the advantages of utilizing aryl alcohols for light absorption *and* proton reduction. This system represents not only a new paradigm for the conversion of light energy into chemical bond energy, but also for the use of aryl alcohol photocatalysts for the production of $H_2$.

**References**

1. J. H. Alstrum-Acevedo, M. K. Brennaman, T. J. Meyer, Chemical Approaches to Artificial Photosynthesis. 2. *Inorg. Chem.* **44**, 6802-6827 (2005).
2. D. K. Dogutan, D. G. Nocera, Artificial Photosynthesis at Efficiencies Greatly Exceeding That of Natural Photosynthesis. *Acc. Chem. Res.* **52**, 3143-3148 (2019).
3. B. Zhang, L. Sun, Artificial photosynthesis: opportunities and challenges of molecular catalysts. *Chem. Soc. Rev.* **48**, 2216-2264 (2019).
4. A. J. Bard, M. A. Fox, Artificial Photosynthesis - Solar Splitting of Water to Hydrogen and Oxygen. *Acc. Chem. Res.* **28**, 141-145 (1995).
5. G. A. N. Felton *et al.*, Review of electrochemical studies of complexes containing the Fe2S2 core characteristic of [FeFe]-hydrogenases including catalysis by these complexes of the reduction of acids to form dihydrogen. *J. Organomet. Chem.* **694**, 2681-2699 (2009).
6. C. Kranz, M. Wächtler, Characterizing photocatalysts for water splitting: from atoms to bulk and from slow to ultrafast processes. *Chem. Soc. Rev.* **50**, 1407-1437 (2021).
7. S. Fukuzumi, Y.-M. Lee, W. Nam, Bioinspired artificial photosynthesis systems. *Tetrahedron* **76**, 131024 (2020).
8. I. McConnell, G. Li, G. W. Brudvig, Energy Conversion in Natural and Artificial Photosynthesis. *Chemistry & Biology* **17**, 434-447 (2010).
9. G. A. N. Felton, R. S. Glass, D. L. Lichtenberger, D. H. Evans, Iron-Only Hydrogenase Mimics. Thermodynamic Aspects of the Use of Electrochemistry to Evaluate Catalytic Efficiency for Hydrogen Generation. *Inorg. Chem.* **46**, 8098-8098 (2007).

10. A. M. Appel, M. L. Helm, Determining the Overpotential for a Molecular Electrocatalyst. *ACS Catal.* **4**, 630-633 (2014).
11. P. Quaino, F. Juarez, E. Santos, W. Schmickler, Volcano plots in hydrogen electrocatalysis - uses and abuses. *Beilstein J. Nanotechnol.* **5**, 846-854 (2014).
12. B. M. Stratakes, A. J. M. Miller, H2 Evolution at an Electrochemical "Underpotential" with an Iridium-Based Molecular Photoelectrocatalyst. *ACS Catal.* **10**, 9006-9018 (2020).
13. K. Maeda, Z-Scheme Water Splitting Using Two Different Semiconductor Photocatalysts. *ACS Catal.* **3**, 1486-1503 (2013).
14. Y. Wang *et al.*, Mimicking Natural Photosynthesis: Solar to Renewable H2 Fuel Synthesis by Z-Scheme Water Splitting Systems. *Chem. Rev.* **118**, 5201-5241 (2018).
15. H.-L. Guo *et al.*, Artificial Photosynthetic Z-scheme Photocatalyst for Hydrogen Evolution with High Quantum Efficiency. *J. Phys. Chem. C* **121**, 107-114 (2017).
16. Y. Sakata, T. Hayashi, R. Yasunaga, N. Yanaga, H. Imamura, Remarkably high apparent quantum yield of the overall photocatalytic H2O splitting achieved by utilizing Zn ion added Ga2O3 prepared using dilute CaCl2 solution. *Chem. Commun.* **51**, 12935-12938 (2015).
17. Z. B. Yu *et al.*, Self-assembled CdS/Au/ZnO heterostructure induced by surface polar charges for efficient photocatalytic hydrogen evolution. *J. Mater. Chem. A* **1**, 2773-2776 (2013).
18. X. Li *et al.*, A review of material aspects in developing direct Z-scheme photocatalysts. *Mater. Today*, doi.org/10.1016/j.mattod.2021.1002.1017 (2021).
19. Z. Yu, F. Li, L. Sun, Recent advances in dye-sensitized photoelectrochemical cells for solar hydrogen production based on molecular components. *Energy Environ. Sci.* **8**, 760-775 (2015).
20. C. Xiang *et al.*, Modeling, Simulation, and Implementation of Solar-Driven Water-Splitting Devices. *Angew. Chem. Int. Ed.* **55**, 12974-12988 (2016).
21. D. S. McClure, N. W. Blake, P. L. Hanst, Singlet-Triplet Absorption Bands in Some Halogen Substituted Aromatic Compounds. *J. Chem. Phys.* **22**, 255-258 (1954).
22. M. S. Lowry *et al.*, Single-Layer Electroluminescent Devices and Photoinduced Hydrogen Production from an Ionic Iridium(III) Complex. *Chem. Mater.* **17**, 5712-5719 (2005).
23. T. J. Whittemore, C. Xue, J. Huang, J. C. Gallucci, C. Turro, Single-chromophore single-molecule photocatalyst for the production of dihydrogen using low-energy light. *Nature Chem.* **12**, 180-185 (2020).
24. M. V. Bobo *et al.*, Bis-Cyclometalated Iridium Complexes Containing 4,4'-Bis(phosphonomethyl)-2,2'-bipyridine Ligands: Photophysics, Electrochemistry, and High-Voltage Dye-Sensitized Solar Cells. *Inorg. Chem.* **59**, 6351-6358 (2020).
25. A. Paul, M. D. Smith, A. K. Vannucci, Photoredox-Assisted Reductive Cross-Coupling: Mechanistic Insight into Catalytic Aryl–Alkyl Cross-Couplings. *J. Org. Chem.* **82**, 1996-2003 (2017).
26. T. S. Teets, D. G. Nocera, Photocatalytic hydrogen production. *Chem. Commun.* **47**, 9268-9274 (2011).
27. L. M. Tolbert, K. M. Solntsev, Excited-State Proton Transfer: From Constrained Systems to "Super" Photoacids to Superfast Proton Transfer. *Acc. Chem. Res.* **35**, 19-27 (2002).
28. A. Kütt *et al.*, A Comprehensive Self-Consistent Spectrophotometric Acidity Scale of Neutral Brønsted Acids in Acetonitrile. *J. Org. Chem.* **71**, 2829-2838 (2006).
29. J. L. Dempsey, J. R. Winkler, H. B. Gray, Mechanism of H2 Evolution from a Photogenerated Hydridocobaloxime. *J. Am. Chem. Soc.* **132**, 16774-16776 (2010).
30. T. Z. Forster, Electrolytic Dissociation of Excited Molecules. *Elektrochem.* **54**, 531-535 (1950).
31. C. Baffert, V. Artero, M. Fontecave, Cobaloximes as Functional Models for Hydrogenases. 2. Proton Electroreduction Catalyzed by Difluoroborylbis(dimethylglyoximato)cobalt(II) Complexes in Organic Media. *Inorg. Chem.* **46**, 1817-1824 (2007).

32. X. Hu, B. S. Brunschwig, J. C. Peters, Electrocatalytic Hydrogen Evolution at Low Overpotentials by Cobalt Macrocyclic Glyoxime and Tetraimine Complexes. *J. Am. Chem. Soc.* **129**, 8988-8998 (2007).
33. K. Izutsu, *Acid-Base Dissociation Constants in Dipolar Aprotic Solvents*. (Blackwell Scientific, Oxford, U.K., 1990).
34. C. G. Margarit, N. G. Asimow, A. E. Thorarinsdottir, C. Costentin, D. G. Nocera, Impactful Role of Cocatalysts on Molecular Electrocatalytic Hydrogen Production. *ACS Catal.* **11**, 4561-4567 (2021).

## Acknowledgments